

Diffractive photon production at high momentum transfer in ep collisions

V. P. Gonçalves* and W. K. Sauter†

High and Medium Energy Group, Instituto de Física e Matemática, Universidade Federal de Pelotas, Caixa Postal 354, CEP 96010-900, Pelotas, Rio Grande do Sul, Brazil

(Received 8 February 2013; published 27 March 2013)

The diffractive photon production at large momentum transfer and large energies is a probe of the parton dynamics of the diffractive exchange. In this paper we revisit the leading order Balitsky-Fadin-Kuraev-Lipatov equation approach for this process and estimate, for the first time, the differential and total cross sections considering the next-to-leading order corrections for the Balitsky-Fadin-Kuraev-Lipatov characteristic function. We obtain a reasonable agreement with the DESY-HERA data.

DOI: [10.1103/PhysRevD.87.054035](https://doi.org/10.1103/PhysRevD.87.054035)

PACS numbers: 12.38.Bx, 13.60.Hb

I. INTRODUCTION

The description of exclusive diffractive processes has been proposed as a probe of the Quantum Chromodynamics (QCD) dynamics in the high energy limit (For recent reviews see, e.g., Ref. [1]). It is expected that the study of these processes provides insight into the parton dynamics of the diffractive exchange when a hard scale is present. In particular, the diffractive vector meson and photon production at large momentum transfer is expected to probe the QCD Pomeron, which is described by the Balitsky-Fadin-Kuraev-Lipatov (BFKL) equation [2–5]. In the last years, the H1 and ZEUS Collaborations at DESY-HERA have measured the exclusive production of ρ , ϕ , J/Ψ and γ with hadron dissociation and large values of $|t|$, the square of the four-momentum transferred across the associated rapidity gap. The experimental data for vector meson production are quite well described in terms of the BFKL formalism at leading order [6–11]. In contrast, for photon production, the analysis presented in Ref. [12] indicates that this approach describes the energy dependence of the cross section, but it is unable to describe its $|t|$ dependence. It is important to emphasize that in Ref. [12] the free parameters present in the BFKL formalism at leading order have been constrained using the experimental data for the total cross section, and the differential cross section was predicted and compared with the data. This procedure is the opposite of that used in Refs. [6,7] in order to describe the vector meson data, where the experimental data for the differential cross section for a fixed energy were used to constrain the free parameters, and the energy dependence of the total cross section was predicted by the LO BFKL equation. The possibility that the use of a different procedure allows us to obtain a better description of the experimental data is our first motivation to revisit the description of the diffractive

photon production in the BFKL formalism. The second one is associated to the fact that in the last years the next-to-leading order (NLO) corrections to the BFKL kernel were determined [13,14] and the origin of the instabilities in the perturbative series was understood and the problem solved using methods based on the combination of collinear and small- x resummations [15–18]. It allows us to include, for the first time, the NLO corrections for the BFKL characteristic function in the analysis of the diffractive photon production at large $|t|$. This is a first step in the direction of a full NLO calculation, since we are not including the NLO corrections to the impact factor associated with the photon-photon transition. It has been calculated in Refs. [19–23], and its analytical form was recently presented in Ref. [24]. Thus, we are aware that our phenomenological study is an educated guess to a complete NLO calculation. However, we hope that this offers some insight into the underlying QCD dynamics.

The paper is organized as follows. In the next section we present a brief discussion about the diffractive photon production at large t in ep collisions. In Sec. III we present the formalism for the calculation of the cross section and the next-to-leading order corrections to the BFKL kernel are briefly revised, as well as the different schemes used to improve the convergence of the perturbative series. In Sec. IV we present our predictions and compare with the available data. Finally, a summary of our main conclusions is presented in Sec. V.

II. DIFFRACTIVE PHOTON PRODUCTION

Diffractive processes such as $ep \rightarrow eXY$, where X and Y are hadronic systems of the dissociated photon and proton, respectively, have been studied extensively at HERA in the last decades (For a recent review see, e.g., Ref. [1]). One of the cleanest of the diffractive processes is that of diffractive photon production ($X = \gamma$), with the final state photon having a large transverse momentum and being well separated in rapidity from the hadronic system Y . The cross

*barros@ufpel.edu.br

†werner.sauter@ufpel.edu.br

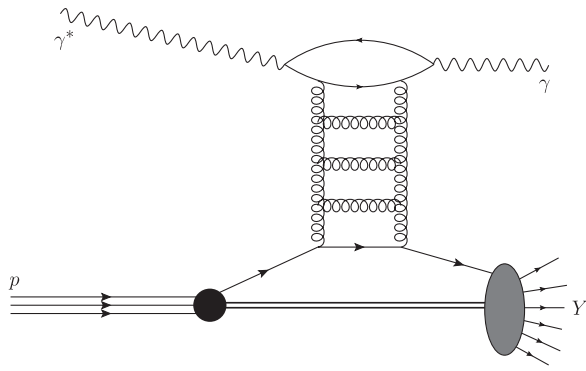


FIG. 1. Diffractive production of a photon with high- t exchange (hard Pomeron) in a virtual photon-proton scattering, producing a hadronic (Y) system.

section for the process of electron-proton scattering measured in HERA is directly related with photon-proton scattering by the relation [12],

$$\frac{d\sigma(ep \rightarrow e + \gamma + Y)}{dQ^2 dy dt} = \Gamma(y, Q^2) \frac{d\sigma(\gamma^* p \rightarrow \gamma + Y)}{dt}, \quad (1)$$

where $y = W^2/s$, W is the center-of-mass energy of the $\gamma^* p$ system and $\Gamma(y, Q^2)$ is the Weizsäcker-Williams approximation of the flux of photons produced by the electron given by [25],

$$\Gamma(y, Q^2) = \frac{\alpha_{\text{em}}}{2\pi} \left[\frac{2m_e^2 y}{Q^4} + \frac{1 + (1-y)^2}{y Q^2} \right]. \quad (2)$$

In the photoproduction regime studied by the H1 Collaboration, this flux is integrated over the range $Q^2 < Q_{\text{max}}^2 = 0.01 \text{ GeV}^2$ [12], which implies

$$\Gamma(y) = \frac{\alpha_{\text{em}}}{2\pi} \left[2m_e^2 y \left(\frac{1}{Q_{\text{max}}^2} \right) + \frac{1 + (1-y)^2}{y} \ln \frac{Q_{\text{max}}^2}{Q_{\text{min}}^2} \right], \quad (3)$$

with $Q_{\text{min}}^2 = m_e^2 y^2 / (1-y)$.

Although parton fragmentation, production of a resolved photon and the Bethe-Heitler process contribute to this process [26], the exchange of gluons in the t channel dominates over the other contributions at large s , which implies that the leading contribution in the high energy regime comes from the Pomeron exchange (See Fig. 1). In this regime, the cross section for the process photon-proton can be fully calculated in the factor impact representation and is given by the convolution of the hard partonic cross section with the parton distribution function in the proton [27–31]. The final expression is

$$\begin{aligned} & \frac{d\sigma(\gamma^* p \rightarrow \gamma + Y)}{dtdx_j} \\ &= \left[\frac{81}{16} G(x_j, |t|) + \sum_j (q_j(x_j, |t|) + \bar{q}_j(x_j, |t|)) \right] \\ & \times \frac{d\hat{\sigma}}{dt}(\gamma^* q \rightarrow \gamma q), \end{aligned} \quad (4)$$

where $G(x_j, |t|)$ and $q_j(x_j, |t|)$ are the gluon and quark distribution functions, respectively, and $d\hat{\sigma}/dt$ is the differential cross section for the subprocess $\gamma^* q \rightarrow \gamma q$. The basic idea is that at large- $|t|$, the gluonic ladder probes a parton inside the target and the struck parton initiates a jet that carries the fraction x_j of the longitudinal momentum of the incoming hadron, being given by $x_j = -t/(-t + M_Y^2 - m^2)$, where M_Y is the mass of the products of the target dissociation and m is the mass of the target. The minimum value of x_j , x_{min} is calculated considering the experimental cuts on M_Y . In what follows we consider a fixed value $x_{\text{min}} = 10^{-2}$ following Ref. [12] and the theoretical studies presented in Refs. [6–11]. Experimentally, in diffractive photon production at large- $|t|$, a backscattering photon is produced with a small angle in the detector, and the transverse momentum of the photon is counterbalanced by the momentum of the jet scattered in the frontal region. The photon and the jet are separated by a large rapidity gap among them.

The diffractive photon production can be modeled in the rest frame of the proton by a sequence of three events: first, the fluctuation of the incoming photon into a quark-antiquark pair a long distance from the proton target; second, the interaction of the pair with the parton q via the exchange of a color singlet state (the gluon ladder); and finally, the annihilation of the final $q\bar{q}$ pair into a real photon. When the ladder interacts with the parton in the proton, it transfers momentum and dissociates the proton, whose fragments hadronize. This process has been studied in Refs. [27–31] and its description is closely related to the diffractive production of vector mesons at large $|t|$, discussed in detail in Refs. [8–11]. The main advantage present in photon production is that the theoretical calculations are simplified by the absence of a vector meson wave function, with the only nonperturbative part being the parton distribution functions of the proton. However, the cross section is suppressed relative to that of vector meson production by the electromagnetic coupling of the $q\bar{q}$ pair to the final state photon. In the next section we present a brief review of the description of this process in the BFKL formalism.

III. BFKL FORMALISM

The energy and momentum transfer dependences of the cross section for the diffractive photon production are directly related to the description of the differential cross section for the partonic process $\gamma^* q \rightarrow \gamma q$, which can be expressed by [29,30],

$$\frac{d\hat{\sigma}}{dt}(\gamma^* q \rightarrow \gamma q) = \frac{1}{16\pi s^2} \{ |\mathcal{A}_{(+,+)}(s, t)|^2 + |\mathcal{A}_{(+,-)}(s, t)|^2 \}, \quad (5)$$

where the scattering amplitudes $\mathcal{A}_{(+,\pm)}$ depend on the polarization states of the photons (represented by the

plus/minus signs) through the impact factors for the transition $\gamma^* \rightarrow \gamma$. As the Pomeron couples directly to the partons in the proton, the scattering amplitude factorizes in the impact factor associated with the transition of the virtual photon into the real photon, the gluonic ladder and the coupling of the Pomeron with the parton in the proton. At leading order the amplitudes are given by [30]

$$\begin{aligned} \mathcal{A}_{(+,+)} &= i\alpha\alpha_s^2 \sum_q e_q^2 \frac{\pi s}{6} \frac{1}{|t|} \int d\nu \frac{\nu^2}{(1/4 + \nu^2)^2} \frac{\tanh(\pi\nu)}{\pi\nu(1 + \nu^2)} \\ &\times \left[\frac{s}{s_0} \right]^{\omega(\nu)} \int_{1/2-i\infty}^{1/2+i\infty} \frac{dz}{2\pi i} \left[\frac{Q^2}{|t|} \right]^{-z/2} \\ &\times \frac{\Gamma(1/2 - i\nu - z/2)\Gamma(1/2 + i\nu - z/2)}{|\Gamma(1/2 + i\nu)|^2} \\ &\times \Gamma(z/2)\Gamma(z/2 + 1)[z^2 + 11 + 12\nu^2], \end{aligned} \quad (6)$$

$$\begin{aligned} \mathcal{A}_{(+,-)} &= i\alpha\alpha_s^2 \sum_q e_q^2 \frac{2\pi s}{3} \frac{1}{|t|} \int d\nu \frac{\nu^2}{(1/4 + \nu^2)^2} \frac{\tanh(\pi\nu)}{\pi\nu(1 + \nu^2)} \\ &\times \left[\frac{s}{s_0} \right]^{\omega(\nu)} \int_{1/2-i\infty}^{1/2+i\infty} \frac{dz}{2\pi i} \left[\frac{Q^2}{|t|} \right]^{-z/2} \\ &\times \frac{\Gamma(3/2 - i\nu - z/2)\Gamma(3/2 + i\nu - z/2)}{|\Gamma(1/2 + i\nu)|^2} \\ &\times \Gamma(z/2)\Gamma(z/2 + 1), \end{aligned} \quad (7)$$

where α is a fine structure constant; α_s is the strong coupling constant (comes from the impact factor and will be kept fixed); e_q is the quark charges; s_0 is an energy scale, chosen to be $c_1 \cdot Q^2 + c_2 \cdot |t|$ (c_1 and c_2 are free parameters) as the meson production case [6] (see discussion below); $\omega(\nu)$ is the BFKL characteristic function; Q^2 is the photon virtuality; and $\Gamma(z)$ is the gamma function. These results have been derived using the Mueller-Tang [32] prescription for the parton-Pomeron coupling and have considered only the contribution associated with the lowest conformal spin ($m = 0$). In Ref. [33] these results have been rederived, and it was shown that the only non-zero contribution for highest conformal spin, $m = 2$, is small. In the photoproduction and large- t regimes of interest in our analysis ($|t| \geq 4 \text{ GeV}^2$), the amplitudes are given by (For details see Ref. [29])

$$\begin{aligned} \mathcal{A}_{(+,+)} &= i\alpha\alpha_s^2 \sum_q e_q^2 \frac{4\pi s}{3} \frac{1}{|t|} \int d\nu \frac{\nu^2}{(1/4 + \nu^2)^2} \frac{\tanh(\pi\nu)}{\pi\nu} \\ &\times \frac{11/4 + 3\nu^2}{1 + \nu^2} \left[\frac{s}{s_0} \right]^{\omega(\nu)}, \end{aligned} \quad (8)$$

$$\begin{aligned} \mathcal{A}_{(+,-)} &= i\alpha\alpha_s^2 \sum_q e_q^2 \frac{4\pi s}{3} \frac{1}{|t|} \int d\nu \frac{\nu^2}{(1/4 + \nu^2)^2} \frac{\tanh(\pi\nu)}{\pi\nu} \\ &\times \frac{1/4 + \nu^2}{1 + \nu^2} \left[\frac{s}{s_0} \right]^{\omega(\nu)}. \end{aligned} \quad (9)$$

The BFKL characteristic function $\omega(\nu)$ is, in general, expressed as follows

$$\omega(\nu) = \bar{\alpha}_s \chi(\gamma), \quad (10)$$

where $\bar{\alpha}_s = (N_c \alpha_s)/\pi$, N_c is the number of colors and $\gamma = 1/2 + i\nu$. The function χ is given at leading order by [2–5]

$$\chi^{\text{LO}}(\gamma) = 2\psi(1) - \psi(\gamma) - \psi(1 - \gamma), \quad (11)$$

where $\psi(z)$ is the digamma function. This characteristic function has been used in Refs. [29–31] in order to estimate the diffractive photon production. However, several shortcomings are present in a leading-order calculation. First, the energy scale s_0 is arbitrary, which implies that the absolute value to the total cross section is therefore not predictable. Second, α_s is not running at LO BFKL. Finally, the power growth with energy violates the s -channel unitarity at large rapidities. Consequently, new physical effects should modify the LO BFKL equation at very large s , making the resulting amplitude unitary. A theoretical possibility for modifying this behavior in a way consistent with the unitarity is the idea of parton saturation [34], where nonlinear effects associated to high parton density are taken into account. Another possible solution, which is expected to diminish the energy growth of the total cross section, is the calculation of higher-order corrections to the BFKL equation. After an effort of several years, the next-to-leading order (NLO) corrections were obtained [13,14], with the χ function being given by

$$\chi(\gamma) = \chi^{\text{LO}}(\gamma) + \bar{\alpha}_s \chi^{\text{NLO}}(\gamma), \quad (12)$$

where the correction term χ^{NLO} is given by [13,14]

$$\begin{aligned} \chi^{\text{NLO}}(\gamma) &= \mathcal{C} \chi^{\text{LO}}(\gamma) + \frac{1}{4} [\psi''(\gamma) + \psi''(1 - \gamma)] \\ &- \frac{1}{4} [\phi(\gamma) + \phi(1 - \gamma)] - \frac{\pi^2 \cos(\pi\gamma)}{4\sin^2(\pi\gamma)(1 - 2\gamma)} \\ &\times \left\{ 3 + \left(1 + \frac{N_f}{N_c^3} \right) \frac{(2 + 3\gamma(1 - \gamma))}{(3 - 2\gamma)(1 + 2\gamma)} \right\} \\ &+ \frac{3}{2} \zeta(3) - \frac{\beta_0}{8N_c} (\chi^{\text{LO}}(\gamma))^2, \end{aligned} \quad (13)$$

where $\mathcal{C} = (4 - \pi^2 + 5\beta_0/N_c)/12$, $\beta_0 = (11N_c - 2N_f)/3$ is the leading coefficient of the QCD β function, N_f is the number of flavors, $\psi^{(n)}(z)$ is the polygamma function, $\zeta(n)$ is the Riemann zeta function and

$$\begin{aligned} \phi(\gamma) + \phi(1 - \gamma) &= \sum_{m=0}^{\infty} \left[\frac{1}{\gamma + m} + \frac{1}{1 - \gamma + m} \right] \\ &\times \left[\psi' \left(\frac{2+m}{2} \right) - \psi' \left(\frac{1+m}{2} \right) \right]. \end{aligned} \quad (14)$$

The main problem associated with these NLO contributions is that they are so large that the problem appears perturbatively unstable. In particular, they imply negative

corrections to the leading-order kernel, resulting in a complex functional structure (pole positions) that gives an oscillating cross section [35]. Moreover, there are also problems associated with the choice of energy scale, the renormalization scheme and related ambiguities.

An alternative to cure the highly unstable perturbative expansion of the BFKL kernel was proposed in Ref. [15], whose authors realized that the large NLO corrections emerge from the collinearly enhanced physical contributions. A method, the ω expansion, was then developed to resum collinear effects at all orders in a systematic way. The resulting improved BFKL equation was consistent with renormalization group requirements through matching to the DGLAP limit and resummation of spurious poles. In this approach the kernel is positive in a much larger region which includes the experimentally accessible one. This approach was revisited in Ref. [18], obtaining an expression for the collinearly improved BFKL kernel, which does not mix longitudinal and transverse degrees of freedom and reproduces very closely the results from Ref. [15]. The characteristic function proposed in Ref. [18], denoted ‘‘All-poles’’ hereafter, is given by

$$\begin{aligned} \omega_{\text{All-poles}} &= \bar{\alpha}_s \chi^{\text{LO}}(\gamma) + \bar{\alpha}_s^2 \chi^{\text{NLO}}(\gamma) \\ &+ \left\{ \sum_{m=0}^{\infty} \left[\left(\sum_{n=0}^{\infty} \frac{(-1)^n (2n)!}{2^n n! (n+1)!} \frac{(\bar{\alpha}_s + a \bar{\alpha}_s^2)^{n+1}}{(\gamma + m - b \bar{\alpha}_s)^{2n+1}} \right) \right. \right. \\ &- \frac{\bar{\alpha}_s}{\gamma + m} - \bar{\alpha}_s^2 \left(\frac{a}{\gamma + m} + \frac{b}{(\gamma + m)^2} - \frac{1}{2(\gamma + m)^3} \right) \left. \right. \\ &\left. + \{\gamma \rightarrow 1 - \gamma\} \right\}, \end{aligned} \quad (15)$$

where

$$a = \frac{5\beta_0}{12N_c} - \frac{13N_f}{36N_c^3} - \frac{55}{36}, \quad b = -\frac{\beta_0}{8N_c} - \frac{N_f}{6N_c^3} - \frac{11}{12}. \quad (16)$$

Another alternative to solve the spurious singularities present in the original NLO kernel was proposed in Ref. [16]. Differently from Refs. [13,14], where the calculations were performed by employing the modified minimal subtraction scheme ($\overline{\text{MS}}$) to regulate the ultraviolet divergences with arbitrary scale setting, in Ref. [16] they propose to solve the energy scale ambiguity using the Brodsky-Lepage-Mackenzie (BLM) optimal scale setting [36] and the momentum space subtraction (MOM) scheme of renormalization. In this approach, the BFKL characteristic function is given by

$$\omega_{\text{BLM}}^{\text{MOM}} = \chi^{\text{LO}}(\gamma) \frac{\alpha_{\text{MOM}}(\hat{Q}^2) N_c}{\pi} \left[1 + \hat{r}(\nu) \frac{\alpha_{\text{MOM}}(\hat{Q}^2)}{\pi} \right], \quad (17)$$

where α_{MOM} is the coupling constant in the MOM scheme,

$$\alpha_{\text{MOM}} = \alpha_s \left[1 + \frac{\alpha_s}{\pi} T_{\text{MOM}} \right], \quad (18)$$

with T being a function of the number of colors, number of flavors and of a gauge parameter (See Ref. [16] for details) and

$$\alpha_s(\mu^2) = \frac{4\pi}{\beta_0 \ln(\mu^2/\Lambda_{\text{QCD}}^2)}. \quad (19)$$

Moreover, the function \hat{Q} is the BLM optimal scale, which is given by

$$\hat{Q}^2(\nu) = Q^2 \exp \left[\frac{1}{2} \chi^{\text{LO}}(\gamma) - \frac{5}{3} + 2 \left(1 + \frac{2}{3} \varrho \right) \right], \quad (20)$$

with $\varrho = -2 \int_0^1 dx \ln(x)/(x^2 - x + 1) \approx 2.3439$. Finally, \hat{r} is the NLO coefficient of the characteristic function,

$$\begin{aligned} \hat{r}(\nu) &= -\frac{\beta_0}{4} \left[\frac{\chi^{\text{LO}}(\nu)}{2} - \frac{5}{3} \right] - \frac{N_c}{4\chi^{\text{LO}}(\nu)} \left\{ \frac{\pi^2 \sinh(\pi\nu)}{2\nu \cosh^2(\pi\nu)} \right. \\ &\times \left[3 + \left(1 + \frac{N_f}{N_c} \right) \frac{11 + 12\nu^2}{16(1 + \nu^2)} \right] - \chi^{\text{NLO}}(\nu) \\ &+ \frac{\pi^2 - 4}{3} \chi^{\text{LO}}(\nu) - \frac{\pi^3}{\cosh(\pi\nu)} - 6\zeta(3) + 4\tilde{\phi}(\nu) \left. \right\} \\ &+ 7.471 - 1.281\beta_0, \end{aligned} \quad (21)$$

with

$$\tilde{\phi}(\nu) = 2 \int_0^1 dx \frac{\cos(\nu \ln(x))}{(1+x)\sqrt{x}} \left[\frac{\pi^2}{6} - \text{Li}_2(x) \right], \quad (22)$$

where $\text{Li}_2(x)$ is the Euler dilogarithm or Spence function.

In Fig. 2 we present a comparison between the distinct BFKL characteristic functions discussed above. For comparison we also present the LO BFKL function. We have that the All-poles and BLM approaches regularize the behavior of the original NLO BFKL characteristic function at small ν and predict similar behaviors for the function ω .

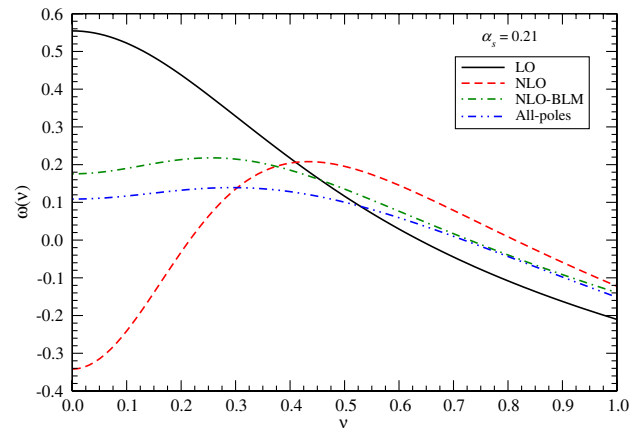


FIG. 2 (color online). ν dependence of the characteristic function obtained considering NLO, NLO + All-poles and NLO + BLM approaches. For comparison, the behavior of the LO BFKL characteristic function is also presented ($\alpha_s = 0.21$).

In particular, the All-poles approach predicts that $\omega(0) = 0.11$, while the BLM one predicts $\omega(0) = 0.18$. As we will show in the next section, this small difference has important implications in the energy dependence of the total cross section for diffractive photon production.

In the next section, we will use Eqs. (11), (15), and (17), as input in Eq. (7) in order to calculate the differential and total cross section in the BFKL formalism.

IV. RESULTS

In this section we present our results for the differential and total cross section and compare our predictions with the H1 experimental data [12]. The differential cross section for the process $\gamma^* p \rightarrow \gamma X$ is given by

$$\frac{d\sigma}{dt} = \int_{x_{\min}}^1 dx_j \frac{d\sigma(\gamma^* p \rightarrow \gamma X)}{dtdx_j}, \quad (23)$$

where we assume that $x_{\min} = 10^{-2}$ following Ref. [12] and previous theoretical studies [6–11]. Moreover, the total cross section is obtained by integration of the Eq. (23) over the $|t|$ -range given by $4.0 \text{ GeV}^2 < |t| < 36.0 \text{ GeV}^2$, according to H1 data [12]. We will use the MSTW2008LO parametrization of the parton distribution functions [37], but we have checked that a different parton parametrization modifies slightly the predictions. In our calculations we have two free parameters: the strong coupling constant and the energy scale parameter s_0 . In what follows we assume that $\alpha_s = 0.21$, which is the value used in Refs. [6–11]. It is important to emphasize that in our calculations α_s is fixed in the impact factors for all approaches studied, since they have been calculated at leading order and running in the characteristic function when we are considering the All-poles and BLM approaches. In contrast to the vector meson production cross section, which is proportional to $\alpha\alpha_s^4$, in the photon production case, it is proportional to $\alpha^2\alpha_s^4$. Following our previous studies [6,7], we have that $s_0 = c_1 \cdot Q^2 + c_2 \cdot |t|$. Considering that the H1 experimental data are for $Q^2 = 10^{-6} \text{ GeV}^2$, we will assume for simplicity that $Q^2 \approx 0$, which implies $s_0 = c_2 \cdot |t|$. Consequently, in our calculations we have only one free parameter: the coefficient c_2 , which will be constrained by the H1 data for the differential cross section as in Refs. [6,7].

In Fig. 3 we present a comparison between our predictions for the differential cross section considering the different approaches for the characteristic function and the H1 data obtained for $Q^2 = 10^{-6} \text{ GeV}^2$ and $W = 219 \text{ GeV}$. We adjust the value of s_0 in order to describe the larger number of experimental points. For the LO BFKL approach we obtain that $c_2 = 10.0$ allow us to describe the data for low and high $|t|$. We have verified that if we adjust the value of s_0 in order to describe the data for $|t| = 12 \text{ GeV}^2$, the LO approach is not able to describe any other data point. In contrast, the value $c_2 = 12.0$ allow us to

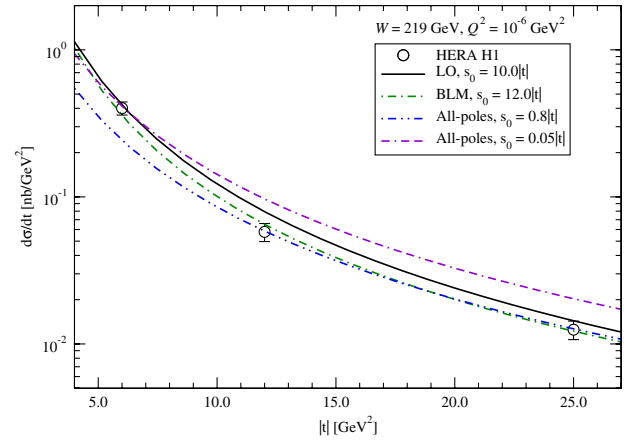


FIG. 3 (color online). Differential cross section for the diffractive photon production at large- t considering differential models for the characteristic function. Experimental data from Ref. [12].

describe all data using the BLM approach. Using the All-poles approach we only describe the data for $|t| > 10 \text{ GeV}^2$ ($c_2 = 0.8$). If we adjust c_2 in order to describe the data for $|t| = 6 \text{ GeV}^2$ ($c_2 = 0.05$) the approach does not describe the experimental data for larger values of $|t|$. Consequently, we can conclude that only the BLM approach allow us to describe all experimental data for the differential cross section. This conclusion also is valid if we consider the value of α_s as a free parameter. In this case the normalization is modified, which implies that a different of c_2 also should be used in order to describe the data, but we have verified that the shape of the $|t|$ dependence is not strongly modified.

Having fixed the free parameter in our calculations, we now are able to predict the energy dependence of the total cross section considering the different approaches for the BFKL characteristic function. In Fig. 4 we present our

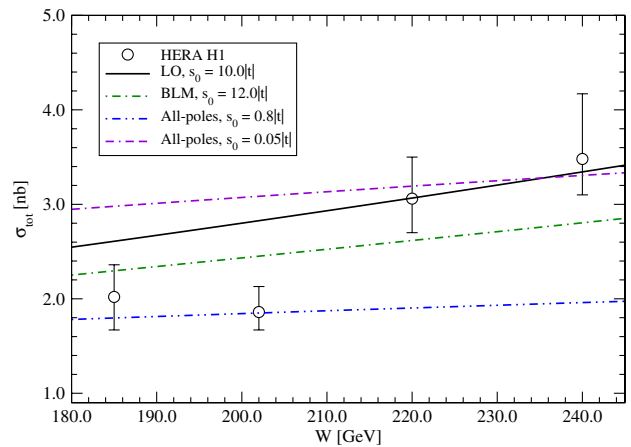


FIG. 4 (color online). Total cross section for the diffractive photon production at large t , considering differential models for the characteristic function. Experimental data from Ref. [12].

predictions. We can see that the LO BFKL approach predicts, as expected, the steeper energy growth of the total cross section. In contrast, the All-poles approach predicts the milder energy dependence. In comparison with the experimental data, any one of the approaches describes all experimental data for the total cross section. The BLM approach, which describes quite well the differential cross section, is able to describe the data at low energy but underestimate the total cross section at high energies. The All-poles prediction is strongly dependent on the parameter c_2 . If $c_2 = 0.8$ is used, this approach describes the data for low energies but underestimates the total cross section at high energies. In contrast, at $c_2 = 0.05$, this approach is only able to describe the data for $W > 210$ GeV.

Some comments are in order before we summarize our main conclusions. First, the current experimental data for the diffractive photon production are scarce and have been obtained in a limited energy range. Certainly, more data and for larger values of energy should allow us to obtain more definitive conclusions about the underlying QCD dynamics. The second, and more important, comment is related to the fact that in our calculations we are using leading order impact factors. In a full NLO calculation one should also consider the NLO corrections to the impact factors. In the last few years, the real and virtual corrections which contributes at NLO has been estimated [19–23] and recently analytical expressions have been proposed [24]. Numerical results were presented in Refs. [23,38] and indicate that the NLO corrections tend to decrease the value of the impact factors. Consequently, our estimates for the total cross section using the NLO-BFKL characteristic functions should be consider an upper bound. It is important to emphasize that the procedure used in our analysis was used in Refs. [39–41] in order to estimate the double production of vector mesons ($\gamma^* \gamma^* \rightarrow VV$) and in Refs. [42,43] to calculate the $\gamma^* \gamma^*$ total cross section. Moreover, in Refs. [44–46], the production of Mueller-

Navelet jets was investigated considering the NLO BFKL kernel and LO impact factors and, more recently, the description of the F_2 structure function has been performed using a similar approach [47–49]. All these studies demonstrate that the study of the diffractive photon production modifying only the BFKL kernel is justified in order to a first estimate of the magnitude of the NLO contributions for this process.

V. SUMMARY

The description of the high energy limit of the Quantum Chromodynamics (QCD) is an important open question in the standard model. During the last decades several approaches were developed in order to improve our understanding from a fundamental perspective. In particular, after a huge theoretical effort, now we have available the NLO corrections for the BFKL characteristic function, which allow us to improve the analysis of the processes that are expected to probe the underlying QCD dynamics. In this paper we have studied, for the first time, the diffractive photon production considering the NLO characteristic functions proposed in Refs. [16,18]. Moreover, the LO BFKL approach for the process was revisited. The free parameters in our calculations have been constrained considering the H1 data for the differential cross section at fixed energy, and the energy dependence of the total cross section has been predicted. We obtain a reasonable description of the scarce experimental data. New data in a large energy range should allow us to obtain more definitive conclusions about the QCD dynamics. Moreover, the inclusion of the NLO correction in the impact factor is an important step that we expect to perform in the near future.

ACKNOWLEDGMENTS

This work was partially financed by the Brazilian funding agencies CNPq and CAPES.

-
- [1] L. Schoeffel, *Prog. Part. Nucl. Phys.* **65**, 9 (2010).
 - [2] L. N. Lipatov, *Sov. J. Nucl. Phys.* **23**, 338 (1976).
 - [3] E. A. Kuraev, L. N. Lipatov, and V. S. Fadin, *Sov. Phys. JETP* **44**, 443 (1976).
 - [4] E. A. Kuraev, L. N. Lipatov, and V. S. Fadin, *Sov. Phys. JETP* **45**, 199 (1977).
 - [5] I. I. Balitsky and L. N. Lipatov, *Sov. J. Nucl. Phys.* **28**, 822 (1978).
 - [6] V. P. Goncalves and W. K. Sauter, *Phys. Rev. D* **81**, 074028 (2010).
 - [7] V. P. Goncalves and W. K. Sauter, *Eur. Phys. J. A* **47**, 117 (2011).
 - [8] J. R. Forshaw and G. Poludniowski, *Eur. Phys. J. C* **26**, 411 (2003).
 - [9] R. Enberg, L. Motyka, and G. Poludniowski, *Eur. Phys. J. C* **26**, 219 (2002).
 - [10] R. Enberg, J. R. Forshaw, L. Motyka, and G. Poludniowski, *J. High Energy Phys.* **09** (2003) 008.
 - [11] G. G. Poludniowski, R. Enberg, J. R. Forshaw, and L. Motyka, *J. High Energy Phys.* **12** (2003) 002.
 - [12] F. D. Aaron *et al.* (H1 Collaboration), *Phys. Lett. B* **672**, 219 (2009).
 - [13] V. S. Fadin and L. N. Lipatov, *Phys. Lett. B* **429**, 127 (1998).
 - [14] M. Ciafaloni and G. Camici, *Phys. Lett. B* **430**, 349 (1998).
 - [15] G. P. Salam, *J. High Energy Phys.* **07** (1998) 019; M. Ciafaloni, D. Colferai, and G. P. Salam, *Phys. Rev. D* **60**, 114036 (1999).

- [16] S.J. Brodsky, V.S. Fadin, V.T. Kim, L.N. Lipatov, and G.B. Pivovarov, *JETP Lett.* **70**, 155 (1999).
- [17] V.A. Khoze, A.D. Martin, M.G. Ryskin, and W.J. Stirling, *Phys. Rev. D* **70**, 074013 (2004).
- [18] A.S. Vera, *Nucl. Phys.* **B722**, 65 (2005).
- [19] V.S. Fadin, D.Y. Ivanov, and M.I. Kotsky, *Nucl. Phys.* **B658**, 156 (2003).
- [20] J. Bartels, S. Gieseke, and C.F. Qiao, *Phys. Rev. D* **63**, 056014 (2001).
- [21] J. Bartels, S. Gieseke, and A. Kyrieleis, *Phys. Rev. D* **65**, 014006 (2001).
- [22] J. Bartels, D. Colferai, S. Gieseke, and A. Kyrieleis, *Phys. Rev. D* **66**, 094017 (2002).
- [23] J. Bartels and A. Kyrieleis, *Phys. Rev. D* **70**, 114003 (2004).
- [24] I. Balitsky and G.A. Chirilli, *Phys. Rev. D* **87**, 014013 (2013).
- [25] S. Frixione, M.L. Mangano, P. Nason, and G. Ridolfi, *Phys. Lett. B* **319**, 339 (1993).
- [26] P. Hoyer, M. Maul, and A. Metz, *Eur. Phys. J. C* **17**, 113 (2000).
- [27] I.F. Ginzburg, S.L. Panfil, and V.G. Serbo, *Nucl. Phys.* **B284**, 685 (1987).
- [28] I.F. Ginzburg and D.Y. Ivanov, *Phys. Rev. D* **54**, 5523 (1996).
- [29] D.Y. Ivanov and M. Wusthoff, *Eur. Phys. J. C* **8**, 107 (1999).
- [30] N.G. Evanson and J.R. Forshaw, *Phys. Rev. D* **60**, 034016 (1999).
- [31] B.E. Cox and J.R. Forshaw, *J. Phys. G* **26**, 702 (2000).
- [32] A.H. Mueller and W.-K. Tang, *Phys. Lett. B* **284**, 123 (1992).
- [33] S. Munier and H. Navelet, *Eur. Phys. J. C* **13**, 651 (2000).
- [34] L.V. Gribov, E.M. Levin, and M.G. Ryskin, *Phys. Rep.* **100**, 1 (1983); F. Gelis, E. Iancu, J. Jalilian-Marian, and R. Venugopalan, *Annu. Rev. Nucl. Part. Sci.* **60**, 463 (2010).
- [35] D.A. Ross, *Phys. Lett. B* **431**, 161 (1998).
- [36] S.J. Brodsky, G.P. Lepage, and P.B. Mackenzie, *Phys. Rev. D* **28**, 228 (1983).
- [37] A.D. Martin, W.J. Stirling, R.S. Thorne, and G. Watt, *Eur. Phys. J. C* **63**, 189 (2009).
- [38] G. Chachamis and J. Bartels, *Proc. Sci.*, DIFF (2006) 026.
- [39] D.Y. Ivanov and A. Papa, *Nucl. Phys.* **B732**, 183 (2006).
- [40] D.Y. Ivanov and A. Papa, *Eur. Phys. J. C* **49**, 947 (2007).
- [41] R. Enberg, B. Pire, L. Szymanowski, and S. Wallon, *Eur. Phys. J. C* **45**, 759 (2006); **51**, 1015(E) (2007).
- [42] V.P. Goncalves, M.V.T. Machado, and W.K. Sauter, *J. Phys. G* **34**, 1673 (2007).
- [43] F. Caporale, D.Y. Ivanov, and A. Papa, *Eur. Phys. J. C* **58**, 1 (2008).
- [44] A.S. Vera and F. Schwennsen, *Nucl. Phys.* **B776**, 170 (2007).
- [45] A.S. Vera, *Nucl. Phys.* **B746**, 1 (2006).
- [46] C. Marquet and C. Royon, *Phys. Rev. D* **79**, 034028 (2009).
- [47] M. Hentschinski, A.S. Vera, and C. Salas, *Phys. Rev. Lett.* **110**, 041601 (2013).
- [48] M. Hentschinski, A.S. Vera, and C. Salas, [arXiv:1301.5283](https://arxiv.org/abs/1301.5283).
- [49] A full NLO BFKL analysis of the Mueller-Navelet jet production was presented in Ref. [50].
- [50] D. Colferai, F. Schwennsen, L. Szymanowski, and S. Wallon, *J. High Energy Phys.* **12** (2010) 026.